INORGANIC CHEMISTRY FRONTIERS

RESEARCH ARTICLE

View Article Online
View Journal | View Issue

Cite this: *Inorg. Chem. Front.*, 2022, **9**, 5688

Decisive role of non-rare earth metals in high-regioselectivity addition of μ_3-carbido clusterfullerene†

Muqing Chen, *‡[a,b] Yaoxiao Zhao,‡[c,f] Fei Jin,[b] Mengyang Li, [c] Runnan Guan,[b] Jinpeng Xin,[b] Yang-Rong Yao,[b] Xiang Zhao, *[c] Guan-Wu Wang, *[d] Qianyan Zhang, *[e] Su-Yuan Xie[e] and Shangfeng Yang *[b]

Endohedral clusterfullerenes featuring encapsulation of metal clusters which transfer electrons to the outer fullerene cages show intriguing chemical properties different from empty fullerenes. Despite the extensive studies on the chemical properties of empty fullerenes, especially C_{60}, chemical functionalization of endohedral clusterfullerenes has been less explored, and previous reports are primarily limited to the well-known metal nitride and carbide clusterfullerenes. Herein, we report the first chemical functionalization of an emerging endohedral clusterfullerene μ_3-carbido clusterfullerene (abbreviated as μ_3-CCF) bearing central μ_3-C and Ti(IV) atoms forming a Ti=C double bond. A μ_3-CCF $Dy_2TiC@I_h$-C_{80} is synthesized, and its molecular structure is unambiguously determined by single-crystal X-ray diffraction for the first time. A photochemical cycloaddition reaction of $Dy_2TiC@I_h$-C_{80} with 2-adamantane-2,3-[3*H*]-diazirine (abbreviated as AdN_2) is then carried out and only one monoadduct $Dy_2TiC@I_h$-C_{80}-Ad is obtained, indicating its high regioselectivity. According to the X-ray single-crystal structure of $Dy_2TiC@I_h$-C_{80}-Ad, the Ad moiety selectively attacks the [6,6]-bond (conjunction of two fused hexagons), which is adjacent to the Ti^{4+} ion instead of the two Dy^{3+} ions, affording a [6,6]-open addition pattern. Theoretical calculations unveil that the Ti(IV) ion plays a decisive role in high regioselectivity, and the formation of [6,6]-open $Dy_2TiC@I_h$-C_{80}-Ad is thermodynamically preferred. Contrarily, a similar reaction of a Ti(III)-containing nitride clusterfullerene $Y_2TiN@C_{80}$ with AdN_2 is predicted to generate a different type of adduct with the addition sites adjacent to the Y^{3+} ion instead of the Ti^{3+} ion. This reveals the peculiarity of the chemical property of μ_3-CCF resulting from the existence of the non-rare earth metal Ti with a high oxidation state.

Received 5th July 2022,
Accepted 7th September 2022

DOI: 10.1039/d2qi01442d

rsc.li/frontiers-inorganic

Introduction

Chemical functionalization of fullerenes offers an opportunity to expand the properties and functionalities of the pristine fullerenes and is essential for applications of fullerene materials in versatile fields such as organic photovoltaic, biomedicine, and catalysis.[1–3] During the past three decades, extensive studies on the chemical properties of empty fullerenes, especially C_{60}, have been reported.[4,5] Upon encapsulating metal clusters into fullerene cages, endohedral clusterfullerenes form and exhibit intriguing chemical properties different from empty fullerenes owing to electron transfer from the encapsulated metal cluster to the outer fullerene cage.[6] Among the known clusterfullerenes, metal nitride and carbide clusterfullerenes were discovered first, and thus their chemical properties have been widely studied.[7–9] Up to now, several different types of chemical reactions, including [2 + 2]-cycloadditions,[10,11] 1,3-dipolar cycloaddition reactions,[12–14] disilylations,[15] Bingel-Hirsch reaction,[16,17] azide addition reac-

[a]*School of Environment and Civil Engineering, Dongguan University of Technology, Dongguan, Guangdong 523808, China. E-mail: mqchen@ustc.edu.cn*
[b]*Hefei National Laboratory for Physical Sciences at Microscale, Key Laboratory of Materials for Energy Conversion, Chinese Academy of Sciences, Department of Materials Science and Engineering, Synergetic Innovation Center of Quantum Information & Quantum Physics, University of Science and Technology of China, Hefei 230026, China. E-mail: mqchen@ustc.edu.cn, sfyang@ustc.edu.cn*
[c]*Institute of Molecular Science & Applied Chemistry, School of Chemistry, Xi'an Jiaotong University, Xi'an 710049, China. E-mail: xzhao@mail.xjtu.edu.cn*
[d]*Hefei National Laboratory for Physical Sciences at Microscale, CAS Key Laboratory of Soft Matter Chemistry, and Department of Chemistry, University of Science and Technology of China, Hefei 230026, China. E-mail: gwang@ustc.edu.cn*
[e]*State Key Lab for Physical Chemistry of Solid Surfaces, Collaborative Innovation Center of Chemistry for Energy Materials, Department of Chemistry, College of Chemistry and Chemical Engineering, Xiamen University, Xiamen 361005, China. E-mail: xmuzhangqy@xmu.edu.cn*
[f]*School of materials science and chemical engineering, Xi'an Technological University, Xi'an 710021, China*

†Electronic supplementary information (ESI) available. CCDC 2036864 and 2036865. For ESI and crystallographic data in CIF or other electronic format see DOI: https://doi.org/10.1039/d2qi01442d

‡These authors contributed equally to this work.

tions,[18] Lewis acid–base addition reactions,[19–21] carbene addition,[22–25] and radical reactions,[26,27] have been applied in functionalizing metal nitride and carbide clusterfullerenes. However, chemical functionalization of other types of endohedral clusterfullerenes has been less explored due mainly to their relatively low yield compared to the metal nitride clusterfullerenes (NCFs) such as $Sc_3N@C_{80}$.

As an emerging endohedral clusterfullerene, the μ_3-carbido cluster-fullerene (abbreviated as μ_3-CCF) discovered in 2014 appears quite special since a non-rare earth (RE) metal such as titanium (Ti) is needed, which bonds with a central μ_3-C atom *via* a Ti=C double bond along with two RE metals.[28] So far, a few Ti-based μ_3-CCFs have been isolated, including $TiM_2C@C_{80}$ (M = Sc, Y, Nd, Gd, Tb, Dy, Er, and Lu)[29–33] and $TiSc_2C@C_{78}$,[29] featuring the electronic configurations of $[Ti^{4+}(M^{3+})_2C^{4-}]^{6+}@C_{2n}{}^{6-}$ involving a Ti^{4+} cation. Noteworthily, this is distinctly different from the conventional metal nitride clusterfullerenes (NCFs) $M_3N@C_{2n}$ in which the encapsulated RE and non-RE metals take formal oxidation states of 3+, affording electronic configurations of $[(M^{3+})_3N^{3-}]^{6+}@C_{2n}{}^{6-}$.[34–36] Thus, an open question arises: given that μ_3-CCFs have similar trimetallic cluster compositions and the same charge state of the outer fullerene cage ($C_{2n}{}^{6-}$) with NCFs, whether are their chemical properties similar to those of NCFs? However, to the best of our knowledge, the chemical functionalization of μ_3-CCFs has never been reported yet, and hence their chemical properties, specifically, the impact of the encapsulated Ti^{4+} cation, remain unknown.

Herein, we report the first chemical functionalization of μ_3-CCF by a cycloaddition reaction of $Dy_2TiC@I_h$-C_{80} with 2-adamantane-2,3-[3*H*]-diazirine (abbreviated as AdN_2). $Dy_2TiC@I_h$-C_{80} is synthesized and its molecular structure is unambiguously determined by single-crystal X-ray diffraction for the first time. After a photochemical reaction of $Dy_2TiC@I_h$-C_{80} with AdN_2, only one monoadduct $Dy_2TiC@I_h$-C_{80}-Ad is obtained, indicating its high regioselectivity. On the basis of the X-ray single-crystal structure of $Dy_2TiC@I_h$-C_{80}-Ad, a [6,6]-open addition pattern is identified. Theoretical calculations are carried out to unveil the role of the Ti^{4+} ion within $Dy_2TiC@I_h$-C_{80} μ_3-CCF in its high regioselectivity.

Results and discussion

Synthesis, isolation and X-ray crystallographic structure of $Dy_2TiC@I_h$-C_{80}

The synthesis procedure of $Dy_2TiC@C_{80}$ by a modified Krätschmer–Huffman DC-arc discharge method is similar to that of $Tb_2TiC@C_{80}$ we reported previously.[32] Isolation of $Dy_2TiC@I_h$-C_{80} was fulfilled by a three-step high performance liquid chromatography (HPLC) procedure, and its high purity was confirmed by matrix-assisted laser desorption ionization time-of-flight (MALDI-TOF) mass spectroscopy and HPLC (see ESI Fig. S1†).

Although $Dy_2TiC@C_{80}$ was reported by Popov *et al.* before,[33] its molecule structure has not been determined unambiguously yet. In this work, we succeeded in determining the molecular structure of $Dy_2TiC@C_{80}$ unambiguously by single-crystal X-ray diffraction for the first time on the basis of growing high-quality cocrystals with decapyrrylcorannulene (DPC) as the host. The relative orientation of $Dy_2TiC@I_h$-C_{80} and two DPC molecules within a 2DPC·{$Dy_2TiC@I_h$-C_{80}} cocrystal is shown in Fig. 1a, which includes only one orientation of the fullerene cage together with the major site of the Dy_2TiC cluster for clarity (see ESI Table S1† for detailed crystallographic data). Similar to other reported clusterfullerene-DPC cocrystals,[37–39] the asymmetric crystal unit cell consists of one pair of fully ordered DPC molecules and one $Dy_2TiC@I_h$-C_{80} molecule.

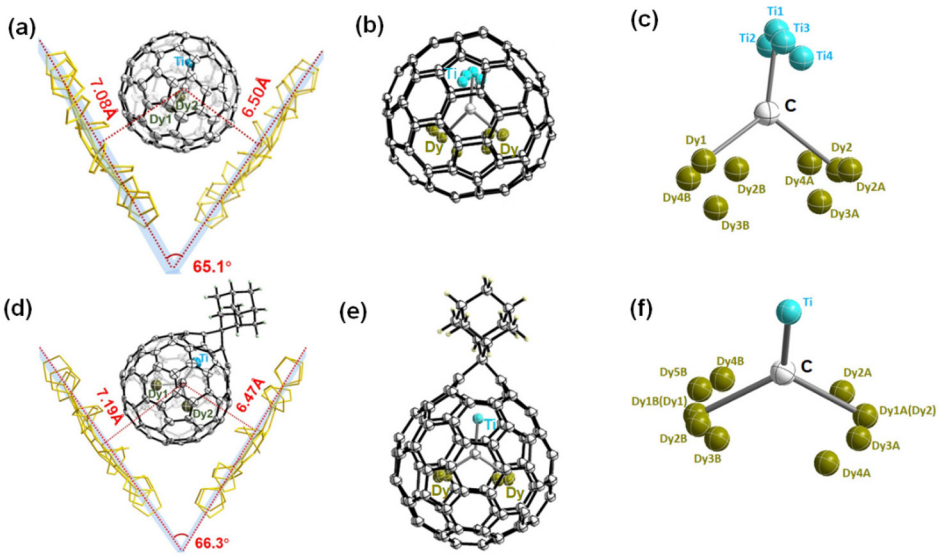

Fig. 1 Crystal structures of (a) 2DPC·{$Dy_2TiC@I_h$-C_{80}} and (d) 2DPC·{$Dy_2TiC@I_h$-C_{80}-Ad}. Geometric configurations of (b) $Dy_2TiC@I_h$-C_{80} and (e) $Dy_2TiC@I_h$-C_{80}-Ad along with the metal positional disorder of the Dy_2TiC cluster within (c) $Dy_2TiC@I_h$-C_{80} and (f) $Dy_2TiC@I_h$-C_{80}-Ad.

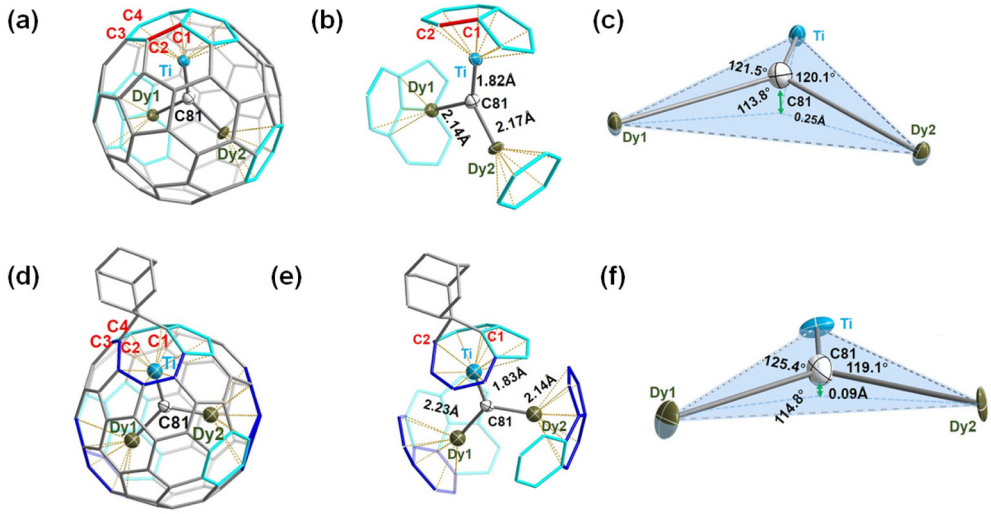

Fig. 2 The crystallographic orientation of the encapsulated Dy_2TiC cluster inside (a and b) $Dy_2TiC@I_h$-C_{80} and (d and e) $Dy_2TiC@I_h$-C_{80}-Ad, as well as (c and f) the configurations of the Dy_2TiC cluster inside both fullerene cages, are also shown. The blue and cyan regions indicate the coordination interactions between the encapsulated metals and the fullerene cage, and the C1–C2 bond is highlighted in red to show the difference before and after the Ad addition.

Meanwhile, two DPC molecules within 2DPC·{$Dy_2TiC@I_h$-C_{80}} exhibit a V-shape geometry with a dihedral angle of 65.1°, and the nearest DPC-C_{80} cage center distances are 7.08 Å/6.50 Å, which is evidently different from that of 2DPC·{$Sc_3N@I_h$-C_{80}} with a dihedral angle of 1.4° and a DPC-C_{80} cage center distance of 6.77/6.77 Å,[39] predicting the distinct electronic configuration of $Dy_2TiC@I_h$-C_{80}, although they share the same I_h-symmetry C_{80} cage.

The ordered I_h-C_{80} cage and the major Dy/Ti sites with the largest occupancies (0.82, 0.91, and 0.80 for Dy1, Dy2, and Ti1, respectively) were extracted from the cocrystal for clarity (ESI Table S2†), showing that the Ti atom is located beneath a [5,6] bond, while the two Dy atoms are positioned beneath a hexagon and a [5,5,6] junction, respectively. Meanwhile, the shortest distances of the encapsulated metals and the outer cage carbons are 2.399 (9) Å, 2.344 (7) Å, and 2.132 (6) Å for Dy1–C75, Dy2–C11, and Ti–C42, respectively (ESI Table S3†), indicating strong metal–cage interactions which were verified by the high occupancy of two Dy atom and one Ti atom disorders. Furthermore, the bond length of Ti–C81 (1.824 (6) Å) is much shorter than those of Dy1–C81 (2.144(6) Å) and Dy2–C81 (2.175(6) Å) (Fig. 2b), indicating the existence of a Ti=C double bond as the characteristic of μ_3-CCF.[28,33] It is intriguing to investigate whether the encapsulated Dy_2TiC cluster takes a planar or pyramidal configuration. We find that the sum value of ∠Dy1–C81–Ti, ∠Dy2–C81–Ti, and ∠Dy1–C81–Dy2 is 355.4° (Fig. 2c), indicating that the encapsulated Dy_2TiC cluster is pyramidal, in which the C81 atom is 0.25 Å deviated from the plane composed of the $TiDy_2$ unit. This is similar to the case of $Tb_2TiC@C_{80}$ but different from the planar cluster found in $Lu_2TiC@C_{80}$, in which the central carbon is 0.07 Å deviated from the trimetallic plane,[28] revealing the influence of the size of RE metal on the geometry of the M_2TiC cluster.

Photochemical reactions of $Dy_2TiC@I_h$-C_{80} with AdN_2

Among the chemical functionalization methods developed for metal nitride and carbide clusterfullerenes, a cycloaddition reaction using AdN_2 as a reagent has been demonstrated to exhibit high reactivity and regioselectivity.[22,24,25,40–43] Hence, in our present work we managed to investigate the cycloaddition reaction of $Dy_2TiC@I_h$-C_{80} μ_3-CCF with AdN_2. The photochemical reaction of $Dy_2TiC@I_h$-C_{80} with AdN_2 is shown in Fig. 3a. A mixture solution of $Dy_2TiC@I_h$-C_{80} and excess AdN_2 in toluene was irradiated with a high-pressure mercury lamp, and the reaction process was monitored by analytical HPLC (Fig. 3b). Before the reaction, the HPLC profile of the pristine mixture solution showed two peaks at 3.6 and 39.8 min which were assigned to the AdN_2/solvent peak and the pristine $Dy_2TiC@I_h$-C_{80}, respectively. After light irradiation

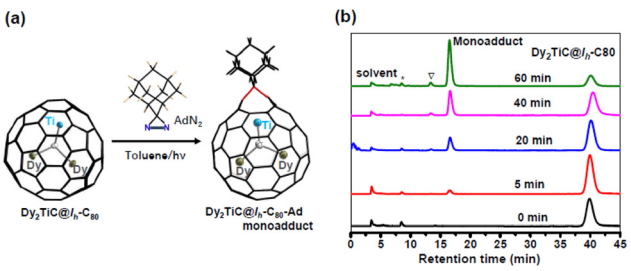

Fig. 3 (a) Synthetic route of $Dy_2TiC@I_h$-C_{80}-Ad through the photochemical reaction of $Dy_2TiC@I_h$-C_{80} with AdN_2; (b) HPLC profiles of the reaction mixtures during the photochemical reaction process of $Dy_2TiC@I_h$-C_{80} with AdN_2 with different reaction times. Conditions: Buckyprep column (⌀ 4.6 mm × 250 mm), 20 μL injection volume, 1.0 mL min^{-1} toluene flow. The inverted triangle and asterisk present the bisadduct and impurity, respectively.

for 5 min, a new peak appeared at 16.5 min, indicating the generation of the monoadduct $Dy_2TiC@I_h$-C_{80}-Ad as confirmed by MALDI-TOF mass spectroscopic characterization. After prolonging the reaction time up to 60 min, the peak at 16.5 min continued to increase along with a decrease of the peak corresponding to the pristine $Dy_2TiC@I_h$-C_{80}, indicating the promoted conversion of $Dy_2TiC@I_h$-C_{80} to the monoadduct $Dy_2TiC@I_h$-C_{80}-Ad. Finally, the reaction was stopped when an obvious peak of bisadduct at 13.3 min appears. Noteworthily, only one monoadduct $Dy_2TiC@I_h$-C_{80}-Ad was obtained even after the reaction proceeded for 60 min, indicating its high regioselectivity. The resultant solution was then subjected to preparative HPLC separation, and the purity of $Dy_2TiC@I_h$-C_{80}-Ad was verified by analytical HPLC (ESI Fig. S2a†). The purified $Dy_2TiC@I_h$-C_{80}-Ad product was characterized by MALDI-TOF mass spectroscopy, showing an intense mass peak at m/z = 1479.8 (ESI Fig. S2b†).

To identify the addition pattern of $Dy_2TiC@I_h$-C_{80}-Ad, we grew high-quality cocrystals using DPC as the host similar to the case of the pristine $Dy_2TiC@I_h$-C_{80}, and successfully determined the molecular structure of $Dy_2TiC@I_h$-C_{80}-Ad unambiguously by single-crystal X-ray diffraction. As illustrated in Fig. 1d, the asymmetric crystal unit cell of the 4DPC·2{$Dy_2TiC@I_h$-C_{80}-Ad} cocrystal contains two pairs of fully ordered DPC molecules and two $Dy_2TiC@I_h$-C_{80}-Ad molecules. DPC molecules within 2DPC·{$Dy_2TiC@I_h$-C_{80}-Ad} exhibit a V-shape geometry with a dihedral angle of 66.3° similar to the pristine 2DPC·{$Dy_2TiC@I_h$-C_{80}} cocrystal and the nearest DPC-C_{80} cage center distances (7.19 Å/6.47 Å) exhibit only minor changes. However, different from the case of the pristine $Dy_2TiC@I_h$-C_{80} with multiple position disorders of Dy and Ti atoms, the encapsulated Ti atom within $Dy_2TiC@I_h$-C_{80}-Ad exhibits no positional disorders while the two Dy atoms still show several disorders (Fig. 1f, Table S2†). This indicates that the attachment of the Ad group between the C1–C2 bond which is fractured effectively traps the underneath Ti atom as a result of the strengthened Ti-cage interaction as discussed in detail below. Furthermore, the main occupancies of the endohedral two Dy atom disorder are 0.42 and 0.43 for $Dy_2TiC@I_h$-C_{80}-Ad, which are obviously less than those (0.82 and 0.91) of pristine $Dy_2TiC@I_h$-C_{80}, suggesting the weakened interaction of Dy atoms and the I_h-C_{80} cage after carbene addition.

According to a close analysis of the single crystal structure of $Dy_2TiC@I_h$-C_{80}-Ad, the Ad moiety selectively attacks the [6,6]-bond (conjunction of two fused hexagons, C1–C2) which is adjacent to the Ti^{4+} ion instead of the two Dy^{3+} ions shown in Fig. 2d and e. Intriguingly, the distance (2.216(2) Å) of the addition sites (C1, C2) is much longer than that of the conventional C–C single bond (1.54 Å), indicating an open-cage addition pattern.[22,41] Hence, a [6,6]-open addition pattern of the Ad moiety can be deduced, which is similar to the cases of photochemical cycloaddition reactions of Ad with metal nitride and carbide clusterfullerenes.[22,24,25,40] Based on the largest occupancy, Dy1, Dy2, and Ti atoms within $Dy_2TiC@I_h$-C_{80}-Ad locate underneath a [5,6] bond, a [5,6]-bond, and a fractured [6,6]-bond, respectively (Fig. 2d and e). It is obvious that Ad addition leads to rotation of the Dy_2TiC cluster from the coordinated blue region to the cyan region (see Fig. 2ab, d and e) due to the self-adaptive interaction between the endohedral cluster and the outer cage. For the encapsulated Dy_2TiC cluster within $Dy_2TiC@I_h$-C_{80}-Ad, the bond lengths of Dy1–C81 (2.242 (5) Å), Dy2–C81 (2.140(5) Å), and Ti–C81 (1.829 (5) Å) are close to those within the pristine $Dy_2TiC@I_h$-C_{80} as discussed above (ESI Table S3†). These results indicate that the μ_3-carbido nature of the encapsulated Dy_2TiC cluster remains unchanged after grafting the Ad moiety. Moreover, the sum value of ∠Dy1–C81–Ti, ∠Dy2–C81–Ti and ∠Dy1–C81–Dy2 becomes 359.3° (Fig. 2f), which is larger than that observed for the pristine $Dy_2TiC@I_h$-C_{80} (355.4°), indicating that the cycloaddition of the Ad moiety to μ_3-CCF induces an obvious geometric change of the encapsulated μ_3-carbido cluster. A plausible explanation is that the grafted Ad moiety results in the deformation of the I_h-C_{80} cage with an enlargement of the confined internal space, and thus the strain of the Dy_2TiC cluster is reduced.[22,24,25,40]

Theoretical calculation of $Dy_2TiC@I_h$-C_{80}-Ad

To understand the high regioselectivity of Ad addition to $Dy_2TiC@I_h$-C_{80} μ_3-CCF and unveil the role of the non-RE metal Ti within the μ_3-carbido cluster, we performed comprehensive theoretical studies. Density functional theory (DFT) computations on the pristine $Dy_2TiC@I_h$-C_{80} μ_3-CCF with S = 5 spin ground state (spin multiple state $2S + 1 = 11$) were carried out, verifying that the encapsulated Dy_2TiC cluster takes a μ_3-carbido structure bearing a Ti^{4+} ion and Ti═C double bond (1.79 Å) (ESI Tables S4–S5, Fig. S3–S4†). Besides, the electronic configuration of $[(Dy^{3+})_2Ti^{4+}C^{4-}]^{6+}@[I_h(31924)$-$C_{80}]^{6-}$ is confirmed similar to the case of the first μ_3-CCF $Lu_2TiC@I_h$-C_{80}.[28]

The high regioselectivity of Ad addition around Ti instead of Dy can be understood by further analyzing the geometric and electronic configuration of $Dy_2TiC@I_h$-C_{80}. First, the shorter Ti–C (cage) distances than those of Dy–C (cage) suggest much stronger interactions between Ti^{4+} with the I_h-C_{80} cage (ESI Table S6†), which is also confirmed by the larger Mayer bond order (MBO), density of electrons, and the Laplacian of the electron density between the Ti^{4+} ion and the I_h-C_{80} cage than those of Dy^{3+} ions with the I_h-C_{80} cage (ESI Tables S6 and S7†). Besides, the Ti^{4+} ion and its adjacent cage carbons with much more negative charges also contribute to the stronger interactions of Ti^{4+}-C (cage) than that of Dy^{3+}-C (cage) (ESI Fig. S4d†).

Considering the simultaneously appeared [5,6]-adduct and [6,6]-adduct isomers in the reaction of $M_3N@I_h$-C_{80} (M = Sc, Lu) with carbene Ad: under light irradiation,[22] it is interesting that our experimental finding shows that only [6,6]-adduct around the Ti^{4+} ion obtained with C1 and C2 as the addition sites instead of C2 and C3 ([5,6]-adduct isomer). The theoretical calculations indicate that the [6,6]-adduct has 3.3 kcal mol^{-1} potential energy (Fig. 4) lower than the [5,6]-adduct. Furthermore, statistical thermodynamic analysis considering the entropy–enthalpy effect shows that [6,6]-open $Dy_2TiC@I_h$-C_{80}-Ad (C1, C2) has the 99.97% distribution relative to that

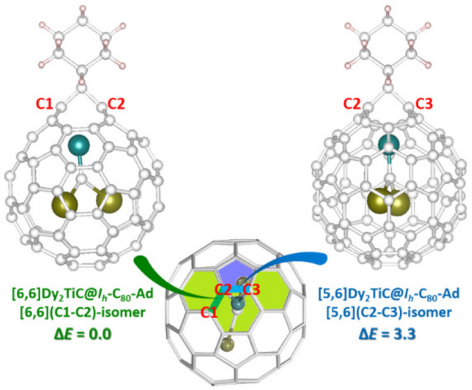

Fig. 4 Relative energies (ΔE, in kcal mol^{-1}) of [5,6]-$Dy_2TiC@I_h$-C_{80}-Ad (in blue) and [6,6]-$Dy_2TiC@I_h$-C_{80}-Ad (in green). The cyan, brown, and light gray balls represent the titanium, dysprosium and carbon atoms, respectively.

(0.03%) of [5,6]-open $Dy_2TiC@I_h$-C_{80}-Ad (C2-C3) at 298.15 K. Thus, the [6,6]-open $Dy_2TiC@I_h$-C_{80}-Ad obtained in experiment is the thermodynamic product, which is the same as the reactions of AdN_2 with several endohedral metallofullerenes previously reported.[23,43]

In order to consolidate the universal role of the Ti(IV) within the μ_3-carbido cluster in determining the regioselectivity and reaction mechanism of μ_3-CCF, we further computed similar cycloaddition products of the analogously reported μ_3-CCF $Y_2TiC@I_h$-C_{80} [33] and nitride clusterfullerene $Y_2TiN@C_{80}$ bearing Ti(III)[44,45] with AdN_2, in which replacing Dy^{3+} with Y^{3+} is to ensure the validity of μ_3-CCF clusterfullerenes. Fig. 5 shows that without the presence of Ti(IV), the Ad moiety of Ti(III)-based [6,6]-$Y_2TiN@I_h$-C_{80}-Ad with the lowest potential energy is located nearly around the Y atom. However, similar to $Dy_2TiC@I_h$-C_{80}-Ad, the Ad moiety selectively attacks the [6,6]-bond of I_h-C_{80} adjacent to the Ti(IV) instead of the Y atom to form a $Y_2TiC@I_h$-C_{80}-Ad adduct with energy superiority. Further frontier molecular orbital (FMO) computations in Fig. S6† show that in the presence of Ti(IV), the FMO occupancy of $Dy_2TiC@I_h$-C_{80} and $Y_2TiC@I_h$-C_{80} are similar to each other (ESI Fig. S5†), but different to that of $Y_2TiN@I_h$-C_{80} bearing Ti(III). This reveals the decisive role of the Ti^{4+} ion with a high formal oxidation state (IV) in the electronic configuration of μ_3-CCF $M_2TiC@I_h$-C_{80}, which directly affects the reactivity. Thus, the cycloaddition reaction of $Y_2TiC@I_h$-C_{80} with AdN_2 is expected to exhibit similar regioselectivity and addition pattern to that of $Dy_2TiC@I_h$-C_{80}.

Effect of Ad addition on the electronic properties of $Dy_2TiC@I_h$-C_{80}

In order to unveil the effect of Ad addition on the electronic properties of $Dy_2TiC@I_h$-C_{80}, we carried out UV-vis-NIR spectroscopic characterization and electrochemical studies (Fig. 6). Their characteristic absorption data and redox potentials along with those of other analogous clusterfullerenes are summarized (ESI Table S8†). The absorption spectrum of $Dy_2TiC@I_h$-C_{80} in the range of 300–1600 nm is featureless, with two broad shoulder peaks at 390 and 676 nm. After grafting an Ad moiety, the shoulder peak at 390 nm becomes more apparent in the absorption spectrum of $Dy_2TiC@I_h$-C_{80}-Ad (Fig. 6a) and the shoulder peak at 676 nm exhibits a negligible change. These results indicate that Ad addition induces little influence on the optical absorption of $Dy_2TiC@I_h$-C_{80}.

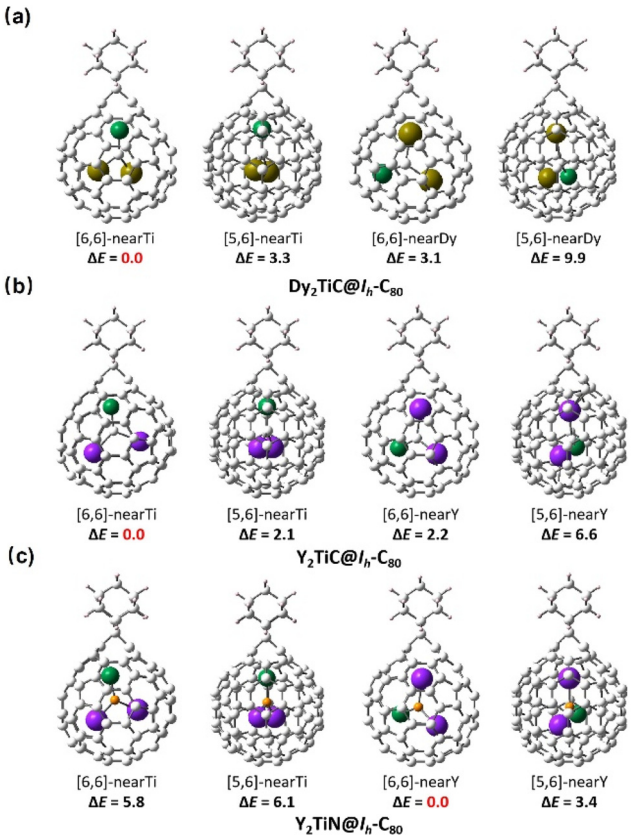

Fig. 5 Relative energies (ΔE, in kcal mol^{-1}) of $Dy_2TiC@I_h$-C_{80} (a), $Y_2TiC@I_h$-C_{80} (b) and $Y_2TiN@I_h$-C_{80} (c) with different addition sites of Ad. The green, brown, purple and light gray balls represent the titanium, dysprosium, yttrium and carbon atoms, respectively.

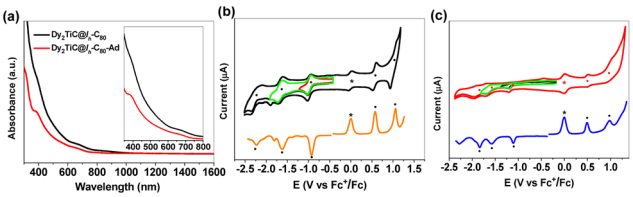

Fig. 6 (a) UV–vis–NIR spectra of $Dy_2TiC@I_h$-C_{80} and $Dy_2TiC@I_h$-C_{80}-Ad dissolved in toluene. Inset: Enlarged spectral region of 350–800 nm. Cyclic voltammograms of (b) $Dy_2TiC@I_h$-C_{80} and (c) $Dy_2TiC@I_h$-C_{80}-Ad in 1,2-dichlorobenzene solution with ferrocene (Fc) as the internal standard under a nitrogen atmosphere. Scan rate: 100 mV s^{-1}, tetrabutylammonium hexafluorophosphate ($TBAPF_6$) as the supporting electrolyte. Each redox step is marked with a solid dot to aid comparison; the asterisk denotes the oxidation peak of ferrocene.

Cyclic voltammometry (CV) and differential pulse voltammetry (DPV) of the pristine $Dy_2TiC@I_h$-C_{80} and $Dy_2TiC@I_h$-C_{80}-Ad are then compared as illustrated in Fig. 6b and c. The pristine $Dy_2TiC@I_h$-C_{80} exhibits two reversible reduction steps, one irreversible reduction step and two reversible oxidation steps which are similar to those reported by Popov *et al.*[33] After Ad addition, all three reduction steps become irreversible, and the first reduction potential shifts negatively from −0.93 V (half-wave potential) to −1.10 V (peak potential), whereas the second and third reduction potentials exhibit a negligible cathodical shift. Only one reversible oxidation step and one irreversible oxidation peak are observed for $Dy_2TiC@I_h$-C_{80}-Ad, with the first oxidation potential cathodically shifting from 0.57 V to 0.49 V relative to that of the pristine $Dy_2TiC@I_h$-C_{80} (ESI Table S8†). This cathodical shift of redox potentials in $Dy_2TiC@I_h$-C_{80} after carbene functionalization is similar to those of Ad adducts of $M_3N@C_{80}$ (M = Sc, Lu) reported previously.[22]

Conclusion

In summary, the first chemical functionalization of μ_3-CCF exemplified by $Dy_2TiC@I_h$-C_{80} is studied, revealing the decisive role of the non-rare earth metal Ti(IV) in high-regioselectivity addition. The molecular structure of the pristine $Dy_2TiC@I_h$-C_{80} is unambiguously determined by single-crystal X-ray diffraction for the first time, revealing the feature of the Ti=C double bond and the influence of the size of rare earth metals on the geometry of the M_2TiC cluster. A photochemical cycloaddition reaction of $Dy_2TiC@I_h$-C_{80} with I_2 affords only one monoadduct $Dy_2TiC@I_h$-C_{80}-Ad, indicating its high regioselectivity. On the basis of the X-ray single crystal structure of $Dy_2TiC@I_h$-C_{80}-Ad, the Ad moiety selectively attacks the [6,6]-bond which is adjacent to the Ti^{4+} ion instead of the two Dy^{3+} ions, and the presence of a [6,6]-open addition pattern is confirmed. According to theoretical calculations, $Dy_2TiC@I_h$-C_{80}-Ad is thermodynamically preferred, and the Ti(IV) ion plays a decisive role in high regioselectivity. In contrast, a similar reaction of a Ti(III)-containing nitride clusterfullerene $Y_2TiN@C_{80}$ with AdN_2 is predicted theoretically to generate a different type of adduct with the addition site adjacent to the Y^{3+} ion instead of the Ti^{3+} ion. Hence, the peculiarity of the chemical properties of μ_3-CCF resulting from the existence of the non-rare earth metal Ti with a high oxidation state is unveiled. As the first chemical functionalization of μ_3-carbido clusterfullerene with high regioselectivity, our finding on the decisive role of non-rare earth metal titanium in the regioselectivity fulfills an in-depth understanding of the fascinating chemical properties of endohedral fullerenes.

Experimental

Detailed experimental process

A toluene solution (25 mL) containing approximately 5 mg of $Dy_2TiC@I_h$-C_{80} and excessive AdN_2 was first degassed for about 15 minutes and later was irradiated with a high-pressure mercury-arc lamp (cutoff <350 nm) at room temperature. The reaction process was monitored by analytical HPLC. The detailed separation procedure of monoadduct $Dy_2TiC@I_h$-C_{80}-Ad using preparative HPLC is presented in the ESI† (LC-908 instrument, Japan Analytical Industry Co., Ltd, toluene as the mobile phase). MALDI-TOF MS was performed on a BIFLEX III (Bruker, Germany) with 1,1,4,4-tetraphenyl-1,3-butadiene (TPB) as the matrix.

Spectroscopic and electrochemical studies

UV-Vis-NIR spectra were recorded on a UV 3150 (Shimadzu, Japan) in toluene. Cyclic voltammetry (CV) and differential pulse voltammetry (DPV) were obtained in 1,2-dichlorobenzene with 0.1 M $(n\text{-}Bu)_4NPF_6$ as the supporting electrolyte using a CHI660E workstation. Pt disc, Pt wire and silver wire were used as the working electrode, reference electrode and auxiliary electrode, respectively. The scan rate for CV was 20 mV s^{-1}. Conditions for DPV: pulse amplitude, 50 mV; scan rate, 20 mV s^{-1}.

X-ray crystallographic study

Crystal blocks of $Dy_2TiC@I_h$-C_{80} and $Dy_2TiC@I_h$-C_{80}-Ad were obtained by slow volatilization of a toluene solution of DPC and $Dy_2TiC@I_h$-C_{80}/$Dy_2TiC@I_h$-C_{80}-Ad in a glass tube. After two weeks, black block crystals suitable for crystal measurements were formed. Single-crystal XRD measurements of $Dy_2TiC@I_h$-C_{80} and $Dy_2TiC@I_h$-C_{80}-Ad crystals were conducted at 100 K at the BL17B station of Shanghai Synchrotron Radiation Facility. The crystal structures were solved with the ShelXT structure solution program using the Intrinsic Phasing method, later refined with the ShelXL[46] refinement package embedded within OLEX2.[47] CCDC 2036864 and 2036865† contain the supplementary crystallographic data for $Dy_2TiC@I_h$-C_{80} and $Dy_2TiC@I_h$-C_{80}-Ad, respectively.

Author contributions

M. C. and Y. Z. contributed equally to this work. M. C. performed the chemical reaction of $Dy_2TiC@C_{80}$ with AdN_2 and confirmed the crystal structures of $Dy_2TiC@C_{80}$ and $Dy_2TiC@C_{80}$-Ad by the crystal growth, crystal measurements and resolution. Meanwhile, M. C. wrote the original draft. Y. Z., M. L. and X. Z. carried out the theoretical calculation and analysis of $Dy_2TiC@C_{80}$ and $Dy_2TiC@C_{80}$-Ad. F. J., J. X. and R. G. synthesized and separated $Dy_2TiC@C_{80}$ for crystal growth and further chemical functionalization. Q. Z. provided decapyrrylcorannulene (DPC) which was used as the host to obtain high-quality single crystals of $Dy_2TiC@C_{80}$ and $Dy_2TiC@C_{80}$-Ad. S. X., G. W. and S. Y. provided the discussion and article revision.

Conflicts of interest

The authors declare no competing financial interest.

Acknowledgements

This work was partially supported by the National Key Research and Development Program of China (2017YFA0402800) and the National Natural Science Foundation of China (52172053, 51925206, 21772189, U1932214, 21773181, 21573172 and 91961113). We thank the staff from BL17B1 at Shanghai Synchrotron Radiation Facility for assistance during data collection. We thank the staff from the BL17B1beamline of the National Facility for Protein Science in Shanghai (NFPS) at Shanghai Synchrotron Radiation Facility, for assistance during data collection.

References

1 R. B. Ross, C. M. Cardona, D. M. Guldi, S. G. Sankaranarayanan, M. O. Reese, N. Kopidakis, J. Peet, B. Walker, G. C. Bazan, E. Van Keuren, B. C. Holloway and M. Drees, Endohedral fullerenes for organic photovoltaic devices, *Nat. Mater.*, 2009, **8**, 208–212.

2 J. Tang, R. Zhang, M. Guo, H. Zhou, Y. Zhao, Y. Liu, Y. Wu and C. Chen, Gd-metallofullerenol drug delivery system mediated macrophage polarization enhances the efficiency of chemotherapy, *J. Controlled Release*, 2020, **320**, 293–303.

3 A. R. Puente Santiago, O. Fernandez-Delgado, A. Gomez, M. A. Ahsan and L. Echegoyen, Fullerenes as Key Components for Low-Dimensional (Photo)electrocatalytic Nanohybrid Materials, *Angew. Chem., Int. Ed.*, 2021, **60**, 122–141.

4 M. D. Tzirakis and M. Orfanopoulos, Radical Reactions of Fullerenes: From Synthetic Organic Chem-istry to Materials Science and Biology, *Chem. Rev.*, 2013, **113**, 5262–5321.

5 M. Yamada, T. Akasaka and S. Nagase, Carbene Additions to Fullerenes, *Chem. Rev.*, 2013, **113**, 7209–7264.

6 S. Yang, T. Wei and F. Jin, When metal clusters meet carbon cages: endohedral clusterfullerenes, *Chem. Soc. Rev.*, 2017, **46**, 5005–5058.

7 P. Jin, Y. Li, S. Magagula and Z. Chen, Exohedral functionalization of endohedral metallofullerenes: Interplay between inside and outside, *Coord. Chem. Rev.*, 2019, **388**, 406–439.

8 M. N. Chaur, F. Melin, A. L. Ortiz and L. Echegoyen, Chemical, electrochemical, and structural properties of endohedral metallofullerenes, *Angew. Chem., Int. Ed.*, 2009, **48**, 7514–7538.

9 X. Lu, L. Feng, T. Akasaka and S. Nagase, Current status and future developments of endohedral metallofullerenes, *Chem. Soc. Rev.*, 2012, **41**, 7723–7760.

10 F.-F. Li, J. R. Pinzon, B. Q. Mercado, M. M. Olmstead, A. L. Balch and L. Echegoyen, [2+2] Cycloaddition Reaction to $Sc_3N@I_h$-C_{80}. The Formation of Very Stable [5,6]- and [6,6]-Adducts, *J. Am. Chem. Soc.*, 2011, **133**, 1563–1571.

11 G.-W. Wang, T.-X. Liu, M. Jiao, N. Wang, S.- E. Zhu, C. Chen, S. Yang, F. L. Bowles, C. M. Beavers, M. M. Olmstead, B. Q. Mercado and A. L. Balch, The cycloaddition reaction of I(h)-Sc3N@C80 with 2-amino-4,5-diisopropoxybenzoic acid and isoamyl nitrite to produce an open-cage metallofullerene, *Angew. Chem., Int. Ed.*, 2011, **50**, 4658–4662.

12 C. M. Cardona, A. Kitaygorodskiy, A. Ortiz, M. A. Herranz and L. Echegoyen, The first fulleropyrrolidine derivative of $Sc_3N@C_{80}$: pronounced chemical shift differences of the geminal protons on the pyrrolidine ring, *J. Org. Chem.*, 2005, **70**, 5092–5097.

13 M. Chen, R. Guan, B. Li, L. Yang, C. Niu, P. Jin, G.-W. Wang and S. Yang, Anomalous Cis-Conformation Regioselectivity of Heterocycle-Fused $Sc_3N@D_{3h}$-C_{78} Derivatives, *Angew. Chem., Int. Ed.*, 2021, **60**, 7880–7886.

14 O. Semivrazhskaya, A. Romero-Rivera, S. Aroua, S. I. Troyanov, M. Garcia-Borras, S. Stevenson, S. Osuna and Y. Yamakoshi, Structures of $Gd_3N@C_{80}$ Prato Bis-Adducts: Crystal Structure, Thermal Isomerization, and Computational Study, *J. Am. Chem. Soc.*, 2019, **141**, 10988–10993.

15 T. Wakahara, Y. Iiduka, O. Ikenaga, T. Nakahodo, A. Sakuraba, T. Tsuchiya, Y. Maeda, M. Kako, T. Akasaka, K. Yoza, E. Horn, N. Mizorogi and S. Nagase, Characterization of the bis-silylated endofullerene $Sc_3N@C_{80}$, *J. Am. Chem. Soc.*, 2006, **128**, 9919–9925.

16 Y. Hu, A. Sole-Daura, Y.-R. Yao, X. Liu, S. Liu, A. Yu, P. Peng, J. M. Poblet, A. Rodriguez-Fortea, L. Echegoyen and F.-F. Li, Chemical Reactions of Cationic Metallofullerenes: An Alternative Route for Exohedral Functionalization, *Chem. – Eur. J.*, 2020, **26**, 1748–1753.

17 T. Cai, L. Xu, C. Shu, H. A. Champion, J. E. Reid, C. Anklin, M. R. Anderson, H. W. Gibson and H. C. Dorn, Selective formation of a symmetric $Sc_3N@C_{78}$ bisadduct: Adduct docking controlled by an internal trimetallic nitride cluster, *J. Am. Chem. Soc.*, 2008, **130**, 2136–2137.

18 T.-X. Liu, T. Wei, S.-E. Zhu, G.-W. Wang, M. Jiao, S. Yang, F. L. Bowles, M. M. Olmstead and A. L. Balch, Azide Addition to an Endohedral Metallofullerene: Formation of Azafulleroids of $Sc_3N@I_h$-C_{80}, *J. Am. Chem. Soc.*, 2012, **134**, 11956–11959.

19 M. Chen, L. Bao, M. Ai, W. Shen and X. Lu, $Sc_3N@I_h$-C_{80} as a novel Lewis acid to trap abnormal N-heterocyclic carbenes: the unprecedented formation of a singly bonded [6,6,6]-adduct, *Chem. Sci.*, 2016, **7**, 2331–2334.

20 M. Chen, W. Shen, P. Peng, L. Bao, S. Zhao, Y. Xie, P. Jin, H. Fang, F.-F. Li and X. Lu, Evidence of Oxygen Activation in the Reaction between an N-Heterocyclic Carbene and $M_3N@I_h(7)$-C_{80}: An Unexpected Method of Steric Hindrance Release, *J. Org. Chem.*, 2017, **82**, 3500–3505.

21 L. Bao, M. Chen, W. Shen, L. Yang, P. Jin and X. Lu, Lewis Acid-Base Adducts of $Sc_2C_2@C_{3v}(8)$-C_{82}/N-Heterocyclic Carbene: Toward Isomerically Pure Metallofullerene Derivatives, *Inorg. Chem.*, 2017, **56**, 14747–14750.

22 M. Yamada, T. Abe, C. Saito, T. Yamazaki, S. Sato, N. Mizorogi, Z. Slanina, F. Uhlik, M. Suzuki, Y. Maeda, Y. Lian, X. Lu, M. M. Olmstead, A. L. Balch, S. Nagase and T. Akasaka, Adamantylidene Addition to $M_3N@I_h$-C_{80} (M=Sc, Lu) and Sc3N@D5h,-C80: Synthesis and Crystallographic Characterization of the [5,6]-Open and [6,6]-Open Adducts, *Chem. – Eur. J.*, 2017, **23**, 6552–6561.

23 M. Yamada, Y. Tanabe, J. Dang, S. Sato, N. Mizorogi, M. Hachiya, M. Suzuki, T. Abe, H. Kurihara, Y. Maeda, X. Zhao, Y. Lian, S. Nagase and T. Akasaka, D_{2d}(23)-C_{84} versus $Sc_2C_2@D_{2d}$(23)-C_{84}: Impact of Endohedral Sc_2C_2 Doping on Chemical Reactivity in the Photolysis of Diazirine, *J. Am. Chem. Soc.*, 2016, **138**, 16523–16532.

24 Y. Iiduka, T. Wakahara, T. Nakahodo, T. Tsuchiya, A. Sakuraba, Y. Maeda, T. Akasaka, K. Yoza, E. Horn, T. Kato, M. T. H. Liu, N. Mizorogi, K. Kobayashi and S. Nagase, Structural determination of metallofullerene Sc_3C_{82} revisited: a surprising finding, *J. Am. Chem. Soc.*, 2005, **127**, 12500–12501.

25 Y. Iiduka, T. Wakahara, K. Nakajima, T. Nakahodo, T. Tsuchiya, Y. Maeda, T. Akasaka, K. Yoza, M. T. H. Liu, N. Mizorogi and S. Nagase, Experimental and theoretical studies of the scandium carbide endohedral metallofullerene $Sc_2C_2@C_{82}$ and its carbene derivative, *Angew. Chem., Int. Ed.*, 2007, **46**, 5562–5564.

26 C. Shu, C. Slebodnick, L. Xu, H. Champion, T. Fuhrer, T. Cai, J. E. Reid, W. Fu, K. Harich, H. C. Dorn and H. W. Gibson, Highly Regioselective Derivatization of Trimetallic Nitride Templated Endohedral Metallofullerenes via a Facile Photochemical Reaction, *J. Am. Chem. Soc.*, 2008, **130**, 17755–17760.

27 N. B. Shustova, A. A. Popov, M. A. Mackey, C. E. Coumbe, J. P. Phillips, S. Stevenson, S. H. Strauss and O. V. Boltalina, Radical trifluoromethylation of $Sc_3N@C_{80}$, *J. Am. Chem. Soc.*, 2007, **129**, 11676–11677.

28 A. L. Svitova, K. B. Ghiassi, C. Schlesier, K. Junghans, Y. Zhang, M. M. Olmstead, A. L. Balch, L. Dunsch and A. A. Popov, Endohedral fullerene with μ3-carbido ligand and titanium-carbon double bond stabilized inside a carbon cage, *Nat. Commun.*, 2014, **5**, 3568.

29 K. Junghans, K. B. Ghiassi, N. A. Samoylova, Q. Deng, M. Rosenkranz, M. M. Olmstead, A. L. Balch and A. A. Popov, Synthesis and Isolation of the Titanium-Scandium Endohedral Fullerenes-$Sc_2TiC@I_h$,-C_{80}, Sc2TiC@D5h-C80 and Sc2TiC2@Ih-C80: Metal Size Tuning of the Ti(IV)/Ti(III) Redox Potentials, *Chem. – Eur. J.*, 2016, **22**, 13098–13107.

30 C. Fuertes-Espinosa, A. Gomez-Torres, R. Morales-Martinez, A. Rodriguez-Fortea, C. Garcia-Simon, F. Gandara, I. Imaz, J. Juanhuix, D. Maspoch, J. M. Poblet, L. Echegoyen and X. Ribas, Purification of Uranium-based Endohedral Metallofullerenes (EMFs) by Selective Supramolecular Encapsulation and Release, *Angew. Chem., Int. Ed.*, 2018, **57**, 11294–11299.

31 A. Brandenburg, D. S. Krylov, A. Beger, A. U. B. Wolter, B. Buchner and A. A. Popov, Carbide clusterfullerene DyYTiC@C_{80} featuring three different metals in the endohedral cluster and its single-ion magnetism, *Chem. Commun.*, 2018, **54**, 10683–10686.

32 F. Liu, F. Jin, S. Wang, A. A. Popov and S. Yang, Pyramidal $TiTb_2C$ cluster encapsulated within the popular I_h(7)-C_{80} fullerene cage, *Inorg. Chim. Acta*, 2017, **468**, 203–208.

33 K. Junghans, C. Schlesier, A. Kostanyan, N. A. Samoylova, Q. M. Deng, M. Rosenkranz, S. Schiemenz, R. Westerstrom, T. Greber, B. Buchner and A. A. Popov, Methane as a Selectivity Booster in the Arc-Discharge Synthesis of Endohedral Fullerenes: Selective Synthesis of the Single-Molecule Magnet $Dy_2TiC@C_{80}$ and Its Congener $Dy_2TiC_2@C_{80}$, *Angew. Chem., Int. Ed.*, 2015, **54**, 13411–13415.

34 M. N. Chaur, R. Valencia, A. Rodriguez-Fortea, J. M. Poblet and L. Echegoyen, Trimetallic Nitride Endohedral Fullerenes: Experimental and Theoretical Evidence for the $M_3N^{6+}@C_{2n}^{(6-)}$ model, *Angew. Chem., Int. Ed.*, 2009, **48**, 1425–1428.

35 J. M. Campanera, C. Bo and J. M. Poblet, General rule for the stabilization of fullerene cages encapsulating trimetallic nitride templates, *Angew. Chem., Int. Ed.*, 2005, **44**, 7230–7233.

36 A. A. Popov and L. Dunsch, Structure, stability, and cluster-cage interactions in nitride clusterfullerenes M3N@C2n (M = Sc, Y; 2n = 68-98): a density functional theory study, *J. Am. Chem. Soc.*, 2007, **129**, 11835–11849.

37 Y. Hu, Y.-R. Yao, X. Liu, A. Yu, X. Xie, L. Abella, A. Rodriguez-Fortea, J. M. Poblet, T. Akasaka, P. Peng, Q. Zhang, S.-Y. Xie, F.-F. Li and X. Lu, Unexpected formation of 1,2- and 1,4-bismethoxyl $Sc_3N@I_h$,-C_{80} derivatives via regioselective anion addition: an unambiguous structural identification and mechanism study, *Chem. Sci.*, 2021, **12**, 8268–8268.

38 F. Jin, J. Xin, R. Guan, X. Xie, M. Chen, Q. Zhang, A. A. Popov, S.-Y. Xie and S. Yang, Stabilizing a three-center single-electron metal-metal bond in a fullerene cage, *Chem. Sci.*, 2021, **12**, 6890–6895.

39 Y.-Y. Xu, H.-R. Tian, S.-H. Li, Z.-C. Chen, Y.-R. Yao, S.-S. Wang, X. Zhang, Z.-Z. Zhu, S.-L. Deng, Q. Zhang, S. Yang, S.-Y. Xie, R.-B. Huang and L.-S. Zheng, Flexible decapyrrylcorannulene hosts, *Nat. Commun.*, 2019, **10**, 485.

40 H. Kurihara, X. Lu, Y. Iiduka, H. Nikawa, N. Mizorogi, Z. Slanina, T. Tsuchiya, S. Nagase and T. Akasaka, Chemical Understanding of Carbide Cluster Metallofullerenes: A Case Study on $Sc_2C_2@C_{2v}$(5)-C_{80} with Complete X-ray Crystallographic Characterizations, *J. Am. Chem. Soc.*, 2012, **134**, 3139–3144.

41 X. Liu, B. Li, W. Yang, Y.-R. Yao, L. Yang, J. Zhuang, X. Li, P. Jin and N. Chen, Synthesis and characterization of carbene derivatives of $Th@C_{3v}$(8)-C_{82} and $U@C_{2v}$(9)-C_{82}: exceptional chemical properties induced by strong actinide-carbon cage interaction, *Chem. Sci.*, 2021, **12**, 2488–2497.

42 W. Zhang, M. Suzuki, Y. Xie, L. Bao, W. Cai, Z. Slanina, S. Nagase, M. Xu, T. Akasaka and X. Lu, Molecular

Structure and Chemical Property of a Divalent Metallofullerene Yb@C_2(13)-C_{84}, *J. Am. Chem. Soc.*, 2013, **135**, 12730–12735.

43 X. Lu, H. Nikawa, L. Feng, T. Tsuchiya, Y. Maeda, T. Akasaka, N. Mizorogi, Z. Slanina and S. Nagase, Location of the yttrium atom in Y@C_{82} and its influence on the reactivity of cage carbons, *J. Am. Chem. Soc.*, 2009, **131**, 12066–12067.

44 C. Chen, F. Liu, S. Li, N. Wang, A. A. Popov, M. Jiao, T. Wei, Q. Li, L. Dunsch and S. Yang, Titanium/Yttrium Mixed Metal Nitride Clusterfullerene TiY_2N@C_{80}: Synthesis, Isolation, and Effect of the Group-III Metal, *Inorg. Chem.*, 2012, **51**, 3039–3045.

45 S. Wang, J. Huang, C. Gao, F. Jin, Q. Li, S.-Y. Xie and S. Yang, Singly Bonded Monoadduct rather than Methanofullerene: Manipulating the Addition Pattern of Trimetallic Nitride Clusterfullerene through One Endohedral Metal Atom Substitution, *Chem. – Eur. J.*, 2016, **22**, 8309–8315.

46 G. M. Sheldrick, Crystal structure refinement with SHELXL, *Acta Crystallogr., Sect. C: Struct. Chem.*, 2015, **71**, 3–8.

47 O. V. Dolomanov, L. J. Bourhis, R. J. Gildea, J. A. Howard and H. Puschmann, OLEX2: a complete structure solution, refinement and analysis program, *J. Appl. Crystallogr.*, 2009, **42**, 339–341.